

# Journal of Biomedical Optics

BiomedicalOptics.SPIEDigitalLibrary.org

## Photoacoustic imaging of lymphatic pumping

Alex Forbrich  
Andrew Heinmiller  
Roger J. Zemp

# Photoacoustic imaging of lymphatic pumping

Alex Forbrich,<sup>a,b,†</sup> Andrew Heinmiller,<sup>b,†</sup> and Roger J. Zemp<sup>a,\*</sup>

<sup>a</sup>University of Alberta, Department of Electrical and Computer Engineering, Edmonton, Alberta, Canada

<sup>b</sup>FUJIFILM VisualSonics, Inc., Toronto, Ontario, Canada

**Abstract.** The lymphatic system is responsible for fluid homeostasis and immune cell trafficking and has been implicated in several diseases, including obesity, diabetes, and cancer metastasis. Despite its importance, the lack of suitable *in vivo* imaging techniques has hampered our understanding of the lymphatic system. This is, in part, due to the limited contrast of lymphatic fluids and structures. Photoacoustic imaging, in combination with optically absorbing dyes or nanoparticles, has great potential for noninvasively visualizing the lymphatic vessels deep in tissues. Multispectral photoacoustic imaging is capable of separating the components; however, the slow wavelength switching speed of most laser systems is inadequate for imaging lymphatic pumping without motion artifacts being introduced into the processed images. We investigate two approaches for visualizing lymphatic processes *in vivo*. First, single-wavelength differential photoacoustic imaging is used to visualize lymphatic pumping in the hindlimb of a mouse in real time. Second, a fast-switching multiwavelength photoacoustic imaging system was used to assess the propulsion profile of dyes through the lymphatics in real time. These approaches may have profound impacts in noninvasively characterizing and investigating the lymphatic system.

© The Authors. Published by SPIE under a Creative Commons Attribution 3.0 Unported License. Distribution or reproduction of this work in whole or in part requires full attribution of the original publication, including its DOI. [DOI: 10.1117/1.JBO.22.10.106003]

Keywords: photoacoustic; lymphatic; lymphatic pumping; imaging systems; multispectral imaging.

Paper 170304R received May 9, 2017; accepted for publication Aug. 15, 2017; published online Oct. 11, 2017.

## 1 Introduction

The lymphatic system, sometimes referred to as “the forgotten second circulation,”<sup>1</sup> plays a crucial role in fluid homeostasis, lipid absorption, and immune system regulation. Compared to the blood circulatory system, the lymphatic system has a unique mechanism for pumping fluids. The peristaltic pumping actions from smooth-muscle lymphangions, as well as the pumping of blood through neighboring blood vessels, help transport fluids through the lymphatic system. Many pathologies directly or indirectly involve the lymphatic system and its pumping mechanisms, often presenting as lymphatic contractile dysfunction, barrier dysfunction, and valve defects.<sup>2</sup> Common clinical procedures, including lymph node resection for cancer diagnostics, sometimes result in morbid complications to the lymphatic system.<sup>2,3</sup> As many as 30% to 50% of breast cancer patients undergoing lymph node or sentinel lymph node dissection develop lymphedema.<sup>4,5</sup> Despite its critical role, the lymphatic system and many of its mechanisms are poorly understood, partly due to the poor contrast of the lymphatic vessels (LVs) and structures. Few imaging techniques are available to visualize the lymphatic system noninvasively *in vivo*, which has significantly hampered our ability to study and understand the lymphatic system.

Lymphography, lymphoscintigraphy, magnetic resonance imaging, positron emission tomography, x-ray computed tomography, and contrast-enhanced ultrasound have all been explored for visualizing the lymphatic system.<sup>6</sup> These imaging techniques require exogenous contrast agents and often are invasive, have poor spatial resolution, or have poor temporal resolution. Recently, near-infrared fluorescence imaging with

indocyanine green (ICG) has been used for lymphography and to visualize lymphatic propulsion and structure, noninvasively, *in vivo*.<sup>6,7</sup> ICG lymphography has shown great promise for the early detection of lymphatic dysfunction,<sup>7</sup> the assessment of lymphedema,<sup>8</sup> and the detection of sentinel lymph nodes in many cancers.<sup>9–11</sup> Near-infrared fluorescence is, however, limited by light scattering and consequently has spatial resolution, which degrades with depth since ballistic photon paths are randomized at depths greater than one transport mean free path (<1 mm).

Photoacoustic imaging is a nascent imaging technique that enables deep tissue imaging while maintaining optical absorption contrast, and its utility for imaging the lymphatic system has been largely unexplored. In brief, photoacoustic imaging relies on the photothermal conversion of pulsed light to heat by optically absorbing molecules causing localized expansion and the subsequent generation of acoustic pressure waves, which can be detected by an ultrasound transducer. Since acoustic waves are scattered 2 to 3 orders of magnitude less than light in tissues, acoustic-resolution photoacoustic imaging enables higher resolution in deep tissues compared to diffuse optical techniques. In acoustic-resolution photoacoustic imaging, the resolution is determined by the characteristics of the acoustic transducer and limited by the ultrasonic diffraction limit. Optical-resolution photoacoustic microscopy of superficial structures is also possible, where the resolution is determined by the optical excitation spot size. By using an exogenous agent, such as methylene blue or ICG, photoacoustic imaging has been used to detect sentinel lymph nodes deep in tissues.<sup>12–14</sup> In 2014, Martel et al.<sup>15</sup> demonstrated an optical-resolution photoacoustic imaging system capable of high spatial and temporal resolution of the lymphatic system. The system was used to image the blood and lymphatic network with micron resolution and to assess the lymphatic flow. Although the optical-resolution photoacoustic

\*Address all correspondence to: Roger J. Zemp, E-mail: rzemp@ualberta.ca

<sup>†</sup>Equally contributing authors

imaging system shows enormous potential and presents impressive vascular and lymphatic structures, only superficial imaging was demonstrated.

To understand and study lymphatic function and mechanisms, it is important to image noninvasively, deep in tissues. As acoustic-resolution photoacoustic imaging tolerates multiply scattered light, it holds significant promise for imaging lymphatic function in deep tissues with high spatial and temporal resolution. Here, we report real-time single-wavelength and multispectral photoacoustic imaging approaches for visualizing lymphatic pumping in murine models in the context of microultrasound anatomical information coregistered with images of blood vessel networks and oxygenation maps. The system was capable of imaging a 14-mm-long cross section through the entire hindlimb (5- to 7-mm deep) with a lateral resolution of 100  $\mu\text{m}$ . Larger fields-of-views and deeper imaging were possible using a different array transducer but were not required for imaging the hindlimb. Multispectral demixing is used to separate an ICG nanoparticle (PAtrace), Evans blue, oxyhemoglobin, and deoxyhemoglobin at 5 frames per second, with capabilities up to 20 frames per second for a limited field-of-view. We believe that this system has great potential in improving our understanding of the lymphatic system, specifically lymphatic pumping. This may improve our understanding of the mechanisms that enable fluid homeostasis and immune cell trafficking.

## 2 Materials and Methods

Ultrasound and photoacoustic imaging were performed using either a Vevo LAZR or Vevo LAZR-X (FUJIFILM VisualSonics Inc.) imaging system. A CD-1 mouse was anaesthetized with isoflurane and setup on a platform that monitored the respiration rate and the heart rate of the mouse. The hair on the hindlimb of the anaesthetized mouse was removed. A 27-G needle catheter was positioned in the footpad of the mouse for injection of the contrast agents. A 30-MHz, linear array ultrasound transducer with integrated fiber optic light delivery (LZ-400 and MX-400, FUJIFILM VisualSonics, Inc.) was positioned longitudinally overtop the hindlimb. Ultrasound imaging was used to make sure that the popliteal lymph node (PLN) was in the field-of-view. The integrated fiber bundle delivered 15 to

20  $\text{mJ}/\text{cm}^2$  of light to the hindlimb of the mouse. Wavelength and pulse-to-pulse energy concentration were applied to account for differences in laser energy. Figure 1(a) shows the position of the needle catheter and the imaging plane. Initially, to visualize lymphatic pumping, photoacoustic imaging was performed at 680 nm before, during, and after a 15- $\mu\text{L}$  bolus injection of either 1.0 mg/mL methylene blue (mouse #1) or 0.1 mg/mL ICG (mouse #2). Image subtraction using preinjection reference images was used to highlight signal changes within the image. After the injection, the transducer was scanned laterally while performing multiwavelength imaging on the same animal to reconstruct a three-dimensional (3-D) image of the methylene blue or ICG-stained lymph nodes. Mouse #1 and #2 were used to visualize the injection of dyes and lymphatic pumping dynamics at the maximum full-width frame rate of 5 Hz and to determine the spectral demixing capabilities of the imaging system.

Another set of experiments performed multiwavelength imaging while a mouse (mouse #3) was injected with a 15- $\mu\text{L}$  bolus of a mixture of Evans blue (0.1 mg/mL) and PAtrace (NanoHybrids, Inc., Austin, Texas, 0.1 mg/mL). PAtrace is a nanoparticle composed of J-aggregates of ICG encapsulated and stabilized by a proprietary biocompatible shell. The shell is PEGylated to enhance circulation time in biological fluids. PAtrace has a neutral, or near zero, zeta potential due to PEG; it is  $90 \pm 20$  nm in diameter with an absorbance maximum at 892 nm. Using the multiwavelength images, the relative concentrations of PAtrace, Evans blue, deoxyhemoglobin, and oxyhemoglobin were demixed using pseudoinverse algorithms available on the Vevo LAZR-X system. Mouse #3 allowed us to visualize differences in the pumping dynamics between two spectrally distinct molecules and to determine the efficacy of a new ICG-based nanoparticle for visualizing the lymphatic system.

The absorption spectra of the contrast agents used in these experiments compared with blood are presented in Fig. 1(b). Multiwavelength experiments used wavelengths of 680, 730, 760, 800, 830, 850, 900, 950, and 970 nm. All animal experiments were conducted in accordance to the protocols set out by the Animal Care and Use Committee at FUJIFILM VisualSonics Inc.

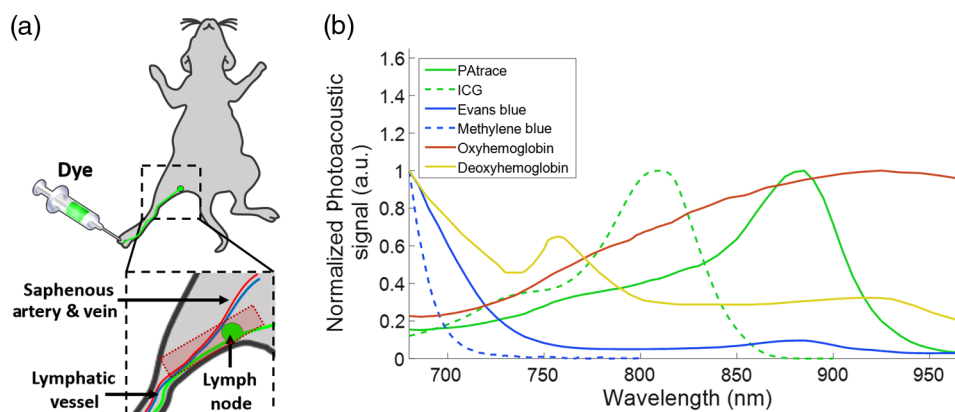


**Fig. 1** (a) Injection site and imaging plane (red shaded area) for visualizing lymphatic pumping. Dye was injected through a 27-G needle catheter placed into the top of the footpad. Ultrasound and photoacoustic imaging were done longitudinally along the hindlimb such that the PLN was visible. (b) Normalized absorption spectra from PAtrace (solid green), ICG (dashed green), Evans blue (solid blue), methylene blue (dashed blue), oxyhemoglobin (red), and deoxyhemoglobin (yellow) (color figure is available online).

### 3 Results and Discussion

Longitudinal photoacoustic imaging of the hindlimb during a 15- $\mu$ L bolus injection of 1.0 mg/mL methylene blue into the footpad of the mouse was used to visualize the flow dynamics of the dye through the lymphatic system. Initially, single-wavelength imaging was used to eliminate the temporal overhead of switching wavelengths and achieve the maximum frame rate of 5 Hz for full-width imaging using the Vevo LAZR imaging system (Fig. 2). Although a significant increase in photoacoustic signal was clearly visible in the PLN [Fig. 2(a)], the location of the dye throughout the image was difficult to assess. Using a series of reference frames taken prior to injection, a different image was formed that highlighted the change in signal [Figs. 2(b) and 2(c)]. The image sequence revealed that dye accumulation occurred in the lymph node, indicating that the dye was indeed being transported through the lymphatic system. The change in photoacoustic signal within regions that represented the PLN, efferent, and afferent LVs, as well as the perilymph node clearly demonstrated the pulsatile nature of the signal within these structures [Figs. 2(d) and 3(e)]. The efferent LV appeared to have a larger signal change; however, we believe this is due to the lymph node having a larger region of interest, which more heavily averages the differential signal. The pumping in the afferent lymph node ranged from 1.5 to 7 pulses per min and did not appear to be correlated to the ECG signals (360

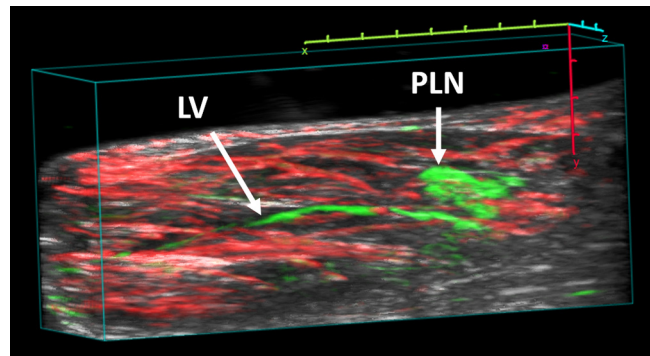


**Fig. 3** Three-dimensional multiwavelength photoacoustic image demixed for ICG and blood (mouse #2, Video 1). The images were demixed from photoacoustic images collected at 680, 730, 760, 800, 830, 850, 900, 950, and 970 nm. The gray, red, and green color-maps represent the ultrasound signal, blood, and relative ICG concentration, respectively. The ICG is isolated to the LV and the PLN. The scale bar represents 1 mm per tick (Video 1, MPEG, 2.2 MB [URL: <http://dx.doi.org/10.1117/1.JBO.22.10.106003.1>]) (color figure is available online).

to 380 beats per min) or the respiration rate (35 to 45 breaths per min), which further indicates that the dyes were being transported through the lymphatic system. Note that the more frequent smaller fluctuations in the signal in the efferent vessel

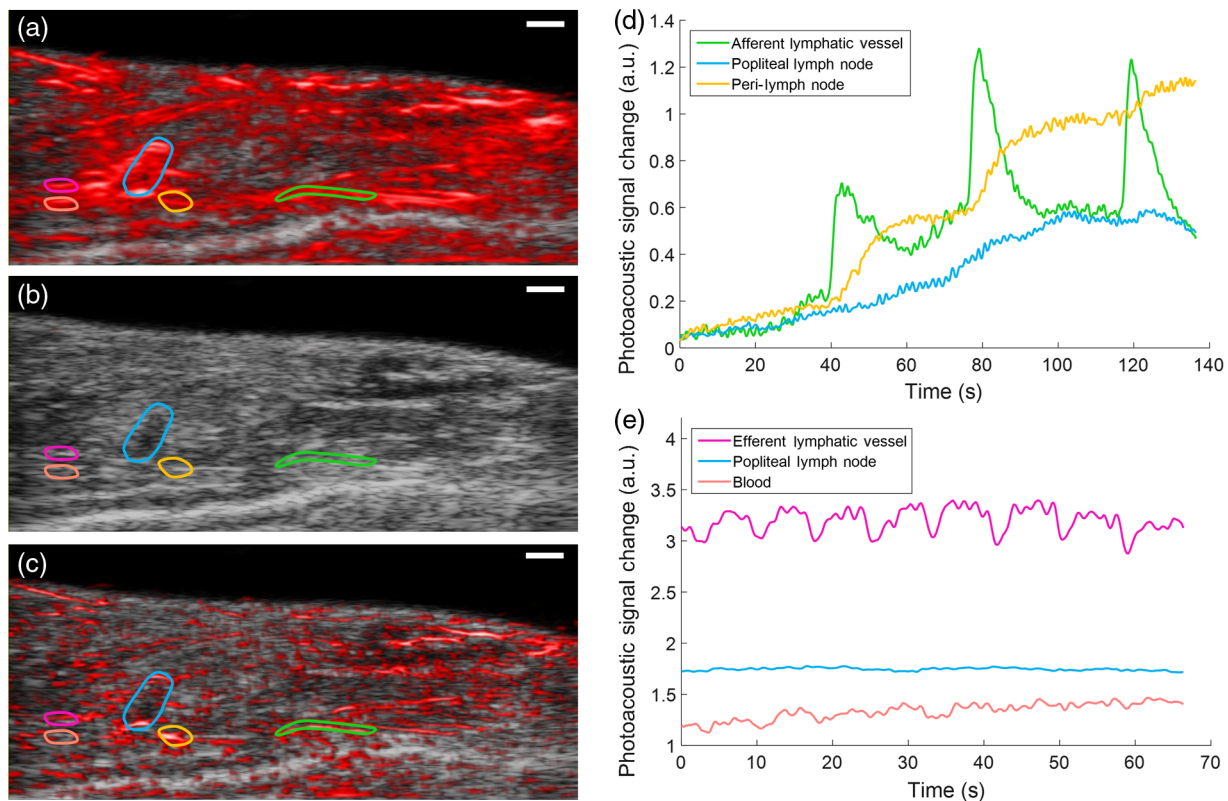


**Fig. 2** Photoacoustic imaging (680 nm) of the PLN during an injection of 1.0 mg/mL methylene blue (mouse #1). Interlaced ultrasound (gray colormap) and photoacoustic (red colormap) imaging of the hindlimb: (a) reference frame for image subtraction, (b) prior to injection, and (c) after injection. The photoacoustic signal in (b) and (c) has the baseline photoacoustic signal removed by subtracting the reference frames. Regions of interest were created surrounding an afferent LV (green), the peri-PLN (orange), the PLN (blue), an efferent LV (pink), and a blood vessel (light red). The white scale bars represent 1 mm. (d) Change in the photoacoustic signal during an injection of methylene blue. (e) Change in the photoacoustic signal in the efferent vessel 10 min after the injection (color figure is available online).

[Fig. 2(e)] appear to be correlated to the respiration rate occurring at a rate of 36 to 42 pulses per min; this may be due to motion briefly moving the LV out-of-plane. The lymphatic pumping rate that we observed is similar to those reported by Kwon and Sevick-Muraca<sup>16</sup> who observed a rate of 0.72 to 11.1 pulses per min. Additionally, the measurements clearly demonstrated that the photoacoustic signal within the lymph node increased after each pulse through the afferent LV indicating the accumulation of methylene blue in the lymph node. As expected, since methylene blue stains lymph nodes, after 10 min, the signal in the lymph node was relatively constant.

To validate the demixing capabilities of the Vevo LAZR imaging system for lymphatic imaging, another mouse was used and injected with 15  $\mu$ L of 0.1 mg/mL ICG into the footpad. Three-dimensional multiwavelength photoacoustic imaging was conducted by laterally moving the LZ-400 transducer at a step size of 0.2 mm over a distance of 5 mm. A constrained pseudoinverse demixing algorithm was used to separate deoxyhemoglobin, oxyhemoglobin, and ICG. Figure 3 shows a 3-D rendering of the hindlimb with blood shown in red and ICG shown in green. The LV and PLN are clearly visible.

As demonstrated in Fig. 3, multiwavelength studies are important to accurately separate the dyes from background signals, such as blood. For longitudinal studies, it is important to image quickly to avoid motion artifacts or, more importantly for these experiments, fluid flow. Using the Vevo LAZR software, the wavelength switching speed takes several hundreds of milliseconds, which may affect these measurements. Since the Vevo LAZR-X has shot-to-shot wavelength-switching capabilities, a higher temporal resolution is achievable potentially increasing the accuracy of spectral demixing. Multiwavelength longitudinal photoacoustic imaging was performed during two injections of a mixture of Evans blue and PATrace. The first injection showed that the contrast agents filled and stained the lymph node and helped align the transducer along the long axis of the LV. Figure 4 shows the results during the second injection. It is interesting to note that longitudinal imaging showed a different propulsion profile for the two different types of dyes. In the afferent LV, the PATrace showed a more discrete propulsion profile compared to Evans blue. The estimated concentration of Evans blue gradually increased over time, whereas the estimated concentration of PATrace changed in bursts and seemed to move

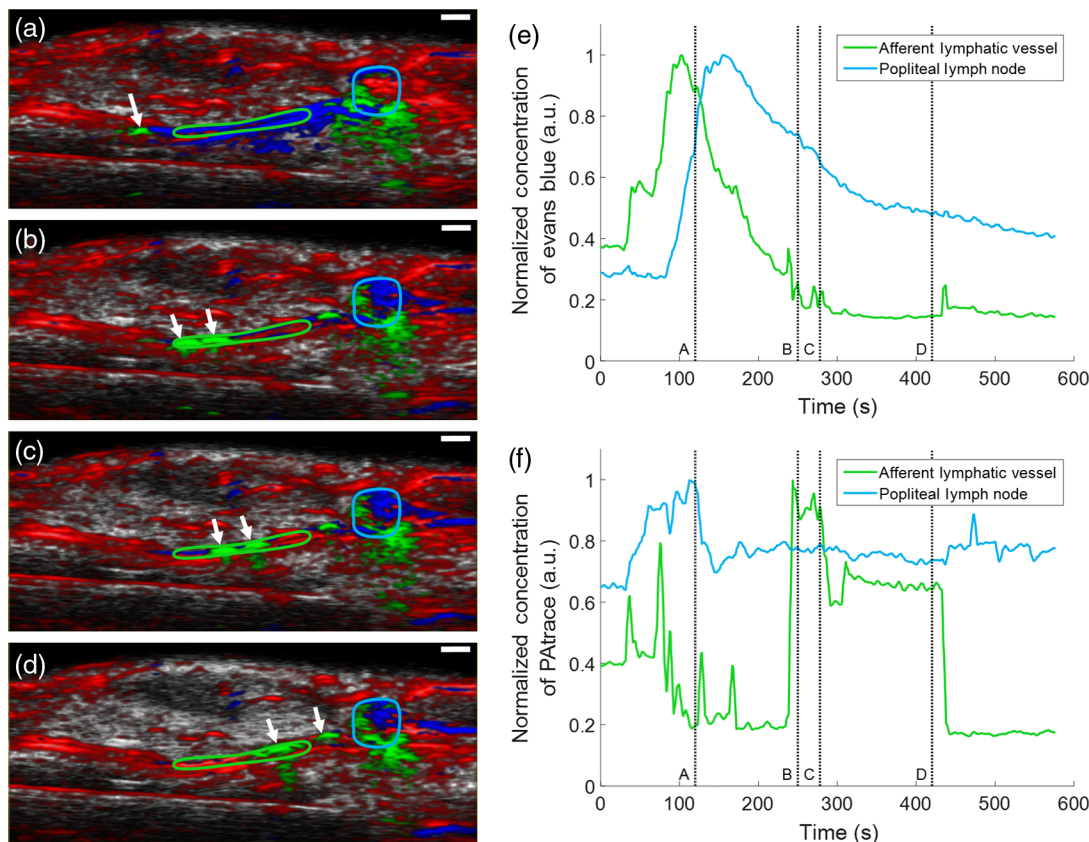


**Fig. 4** Demixed photoacoustic image of lymphatic pumping in the hindlimb of a mouse (mouse #3, Video 2). The images were demixed from photoacoustic images collected at 680, 730, 760, 800, 830, 850, 900, 950, and 970 nm. Evans blue and PATrace were coinjected into the footpad of a mouse. (a–d) represent still frames during the injection at 120, 250, 280, and 420 s, respectively. The relative concentration of PATrace, Evans blue, and blood is presented as the green, blue, and red color-maps, respectively. The white scale bars represent 1 mm. For clarity, Fig. 5 shows the still frames for each of the individual component at the time points indicated in (a–d). (e) Relative demixed concentration estimates of Evans blue in the afferent LV (green) and the PLN (blue). (f) Relative concentration estimates of PATrace in the afferent LV (green) and the PLN (blue). The timepoints for the still frames are marked by vertical lines in (e) and (f). (Video 2, MPEG, 10.6 MB [URL: <http://dx.doi.org/10.1117/1.JBO.22.10.106003.2>]) (color figure is available online).

between different compartments along the LV, which may be indicative of the lymphangions in the vessel. Although the difference in pumping rates is not well-understood, it may be due to the lipophilic nature of the PAttrace nanoparticle compared to the hydrophilic nature of Evans blue and the high affinity of Evans blue to serum albumin. The larger size of the PAttrace nanoparticle may also affect the transportation of the contrast agent through the LV and may cause the agent to be trapped in the lymph node. This hypothesis may explain why the PAttrace signal did not decrease in the lymph node [Fig. 4(f)]. As this was the second injection of the contrast agents, it is noteworthy that the PAttrace nanoparticle seemed to remain in the lymph node while the Evans blue stained the lymph node and some of the excess drained out the node resulting in an initial rise and fall in Evans blue concentration [Fig. 4(e)].

This paper represents one of the first reports using a commercial, high-resolution photoacoustic imaging system to visualize lymphatic pumping at depths 3- to 5-mm deep. With this system and the LZ-400 or MX-400 (18- to 38-MHz linear array transducer), we were able to image 150- to 250- $\mu\text{m}$ -diameter LVs and 3.5-mm deep in tissues. Although optical-resolution photoacoustic imaging has been used to visualize much smaller LVs with higher resolution, the depth capabilities of such systems are substantially limited.<sup>15</sup> Planar fluorescent imaging is capable of deep imaging, however, the spatial resolution of the system presented here (110  $\mu\text{m}$ ) is significantly finer than fluorescent imaging at comparable depths. Finally, our field-of-view is more limited than intensified CCD camera-based near-infrared imaging; however, our approach provides volumetric depth resolution imaging capabilities.

The spectral demixing results demonstrated in Fig. 4 only show the relative concentration of the components. This is

adequate to understand the pumping profile of the lymphatic network and may be useful for some lymphatic disorders. It cannot, however, enable the absolute quantification of the contrast agents, which is important for assessing the concentration within the sentinel lymph nodes, specifically for contrast agents that are targeted to cancer metastasis biomarkers. Although beyond the scope of this work, it would be theoretically possible to use spectral demixing techniques to perform absolute quantification of, at least, the ICG dye where the absorption spectrum is dependent on concentration. This would require more robust fluence correction algorithms to more accurately determine the photoacoustic spectra at each location within the image.

Since these experiments used bolus injections of the dyes, there may have been higher pressures in the lymphatic system causing more rapid drainage initially. Additional studies should investigate lymphatic pumping and flow using a slow, continuous intradermal injection of the dye. More work is needed to understand the reason for the differing pumping rates of dyes. Additionally, more work should investigate the minimum concentration of the dyes required for adequate visualization of lymphatic structures.

Future work should consider combining the wide field-of-view of intensified near-infrared CCD imaging of lymphatic flow<sup>6,7</sup> with the presented high-resolution depth-resolved system for a more detailed view of lymphatic regulation and dysfunction. Future work should also focus on improving depth of imaging for clinical applications, where lymph nodes can be deeper in tissues. This should be possible given recent demonstrations of photoacoustic imaging at multiple-centimeter depths using lower-frequency transducers. The present study using high-frequency ultrasound transducers is well-suited to preclinical applications.

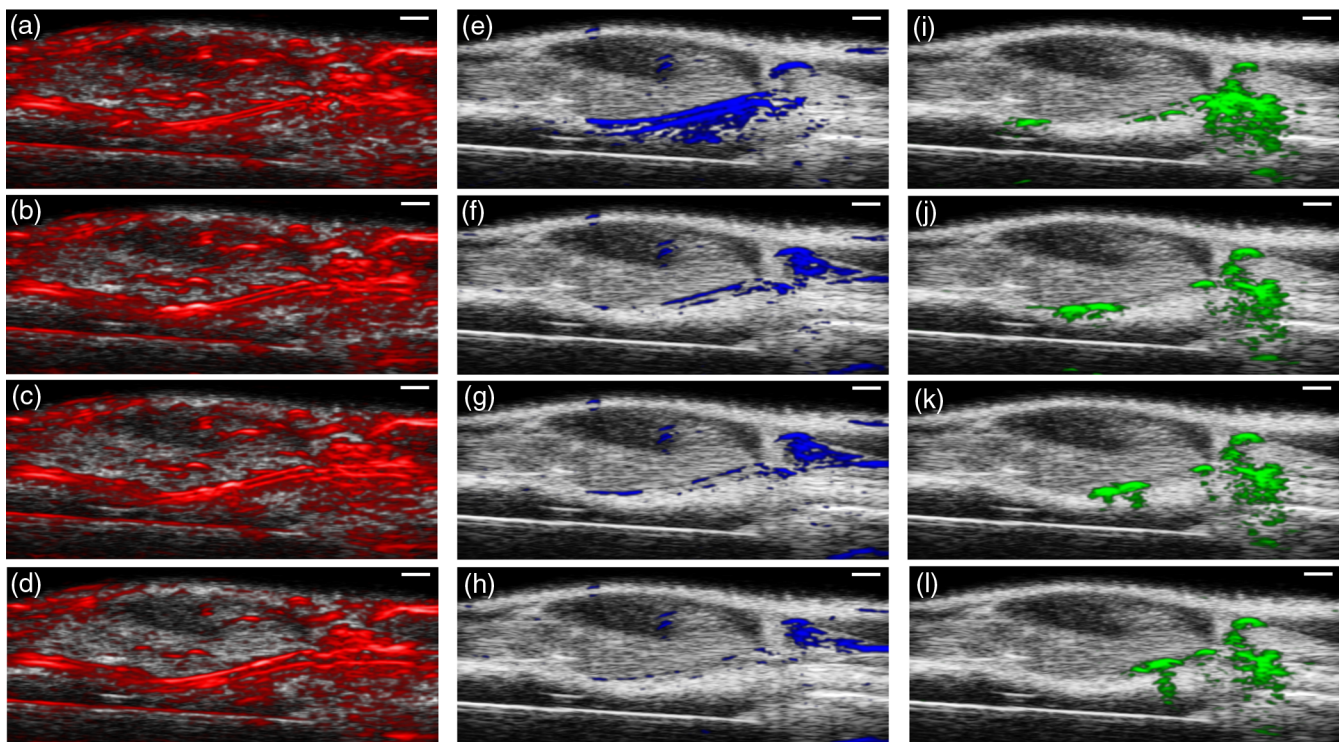


**Fig. 5** Demixed photoacoustic images of lymphatic pumping in the hindlimb of a mouse. Evans Blue and PAttrace were coinjected into the footpad of a mouse. Still frames depicting the relative concentration of blood (A-D, red colormap), Evans Blue (E-H, blue colormap), and PAttrace (I-L, green colormap) are overlaid on the ultrasound image (gray colormap). The white scalebars represent 1 mm.

Given so many unanswered questions about the lymphatic system, we believe this approach may provide an innovative toolset for understanding lymphatic function. This may lead to image-guided intervention to mitigate some morbid side-effects of lymph node resection. It may also contribute to new research capabilities for treating lymphedema and related diseases and may improve our understanding of lymphatic system pathogenesis. Additionally, we believe that the results of the injection of multiple contrast agents and spectral demixing provide a proof-of-concept basis for future work that can use multiple targeted contrast agents to visualize distinct characteristics of the lymphatic system simultaneously and noninvasively, *in vivo*.

#### 4 Conclusion

We have demonstrated photoacoustic imaging of lymphatic pumping with 110- $\mu\text{m}$  resolution at depths of up to 5 mm. The system is capable of shot-to-shot wavelength switching enabling multiwavelength, spectroscopic imaging of PAttrace, Evans blue, and methylene blue at frame rates suitable for imaging peristaltic flow in LVs. These capabilities may enable toolsets for researchers and clinicians in understanding and treating lymphatic disorders.

#### Disclosures

The authors declare no competing financial interests.

#### Acknowledgments

We gratefully acknowledge NanoHybrids for providing the PAttrace contrast agent used in these experiments.

#### References

1. L. Adamczyk et al., "Lymph vessels: the forgotten second circulation in health and disease," *Virchows Arch.* **469**(1), 3–17 (2016).
2. J. Scallan et al., "Lymphatic pumping: mechanics, mechanisms and mal-function," *J. Physiol.* **594**(20), 5749–5768 (2016).
3. R. Ahmed et al., "Risk factors for lymphedema in breast cancer survivors, the Iowa women's health study," *Breast Cancer Res. Treat.* **130**(3), 981–991 (2011).
4. Y. Cemal, A. Pusic, and B. Mehrara, "Preventative measures for lymphedema: separating fact from fiction," *J. Am. Coll. Surg.* **213**(4), 543–551 (2011).
5. J. Armer, "The problem of post-breast cancer lymphedema: impact and measurement issues," *Cancer Invest.* **23**(1), 76–83 (2005).
6. L. Munn and T. Padera, "Imaging the lymphatic system," *Microvasc. Res.* **96**, 55–63 (2014).
7. M. Marshall et al., "Near-infrared fluorescence imaging in humans with indocyanine green: a review and update," *Open Surg. Oncol. J.* **2**(2), 12–25 (2010).
8. M. Aldrich et al., "Lymphatic abnormalities in the normal contralateral arms of subjects with breast cancer-related lymphedema as assessed by near-infrared fluorescent imaging," *Biomed. Opt. Express* **3**(6), 1256–1265 (2012).
9. Y. Ogasawara et al., "Evaluation of breast lymphatic pathways with indocyanine green fluorescence imaging in patients with breast cancer," *World J. Surg.* **32**(9), 1924–1929 (2008).
10. E. Sevick-Muraca et al., "Imaging of lymph flow in breast cancer patients after microdose administration of a near-infrared fluorophore: feasibility study," *Radiology* **246**(3), 734–741 (2008).
11. J. van der Vorst et al., "Dose optimization for near-infrared fluorescence sentinel lymph node mapping in patients with melanoma," *Br. J. Dermatol.* **168**(1), 93–98 (2013).
12. K. H. Song et al., "Noninvasive photoacoustic identification of sentinel lymph nodes containing methylene blue *in vivo* in a rat model," *J. Biomed. Opt.* **13**(5), 054033 (2008).
13. A. Garcia-Urbe et al., "Dual-modality photoacoustic and ultrasound imaging system for noninvasive sentinel lymph node detection in patients with breast cancer," *Sci. Rep.* **5**, 15748 (2015).
14. D. Grootendorst et al., "First experiences of photoacoustic imaging for detection of melanoma metastases in resected human lymph nodes," *Lasers Surg. Med.* **44**(7), 541–549 (2012).
15. C. Martel et al., "Photoacoustic lymphatic imaging with high spatial-temporal resolution," *J. Biomed. Opt.* **19**(11), 116009 (2014).
16. S. Kwon and E. Sevick-Muraca, "Noninvasive quantitative imaging of lymph function in mice," *Lymphatic Res. Biol.* **5**(4), 219–232 (2007).

Biographies for the authors are not available.